

Paramagnetic Effect in Superconductors. VI. Resistance Transitions in Indium Wires

HANS MEISSNER AND RICHARD ZDANIS

The Johns Hopkins University, Baltimore, Maryland

(Received July 19, 1957)

The resistance of indium wires from 0.04 to 2 mm in diameter has been measured as a function of the current, in the temperature region 2.9 to 4.2°K. The samples had residual resistance ratios $r_0 = R_0^{\circ\text{K}}/R_0^{\circ\text{C}}$ of 2 to 7×10^{-4} . For all samples, the transition curves measured showed a steep rise with a break at the critical current. The ratio of critical resistance to the normal resistance is examined as a function of temperature, electronic mean free path and sample diameter. Corrections are made for the temperature and magnetic-field dependence of the resistivity.

I. INTRODUCTION

THIS investigation was conducted as an extension of the research carried out in this laboratory on tin,¹ referred to as part V, and the analysis of these data closely parallels that of part V.

The experimental arrangement is the same as that described in part V.

II. SAMPLES

The samples were prepared from 99.97% pure indium purchased from the Indium Corporation of America.

Samples I, II, III, VI, and IX (0.176 mm $\leq d \leq$ 1.936 mm) were extruded wires. All except IX were electrolytically polished by the following method: the electrolyte consisted of 2 parts absolute methyl alcohol and 1 part concentrated nitric acid, the bath being cooled with dry ice. An indium cathode was used. The voltage drop between the sample and the cathode was adjusted to about 4 volts, just under the voltage where the brown boundary layer of the electrolyte is broken by bubbles.²

Sample III, which was stored at room temperature for ten weeks after extrusion, had the appearance of a single crystal when etched.

Sample IV was a single crystal grown in a thick-walled glass capillary similar to the smaller tin single crystals.¹

Sample VI was an extruded wire of 0.314-mm diameter which was electrolytically etched² to 0.176-mm diameter.

Samples XI, XII, and XIII were drawn in glass. The procedure was to seal indium in a piece of glass tubing, heat the glass until pliable and draw it into a thin capillary. The very thin wire of indium thus obtained was freed of its glass sheath by etching with hydrofluoric acid.

The current and potential leads for all samples except XI, XII, and XIII were soldered in place with In-Sn solder (a mixture of 94% In and 6% Sn by weight), care being taken to attach the potential taps with the least possible disturbance to the sample.

Sample IX was mounted vertically in a copper tube.

The copper tube was used as a current return and was necessary for this sample because the disturbing field, due to leads, became an appreciable portion of the critical magnetic field. (The ratio H_d/H_c , where H_d is the disturbing magnetic field and H_c is the critical magnetic field, is directly proportional to the diameter of the sample. Thus the return tube was only necessary for the sample of largest diameter.)

The current and potential leads for samples XI, XII, and XIII were pressed into place, since indium can readily be joined by moderate pressure at room temperature.

Table I lists the diameter, length, ice-point resistance, and residual resistance ratio of all samples. The residual resistance ratio listed in Table I includes both impurity resistance and the effects of boundary scattering. Since boundary scattering is observed, it is possible to calculate the electronic mean free path for our indium samples.

The ratio $1/\rho l$, where ρ is the resistivity and l is the electronic mean free path, was obtained by using the equation

$$\rho_0 = \rho_{00}(1 + al/d), \quad (1)$$

where ρ_{00} is the impurity resistivity, d is the sample diameter, and a is a constant, less than 1.045, depending on the degree of elastic scattering of the electrons. In Fig. 1 the residual resistance ratio is plotted as a func-

TABLE I. Data on indium samples.

Sample No.	Diameter (mm)	Distance between potential taps (mm)	Ice-point resistance (milliohms)	Residual resistance ratio 10%
I ^a	1.11	40	3.26	5.46
II ^a	0.608	40.5	11.5	6.46
III ^b	0.314	41.2	41.8	2.11
IV ^c	1.140	31.1	2.56	1.58
VI ^d	0.176	3.035	10.99	3.61
IX ^e	1.936	40.8	1.114	1.84
XI ^f	0.038	5.9	445	5.71
XII ^f	0.062	10.5	310	4.96
XIII ^f	0.069	17.7	587	5.02

^a Extruded wire.

^b Extruded wire which looked like a single crystal.

^c Single crystal.

^d Extruded wire etched down.

^e Extruded wire in copper return tube.

^f Drawn in glass.

¹ Hans Meissner, preceding paper [Phys. Rev. **109**, 668 (1958)].

² G. Kehl, *Principles of Metallographic Laboratory Practice* (McGraw-Hill Book Company, Inc., New York, 1949), pp. 27-31.

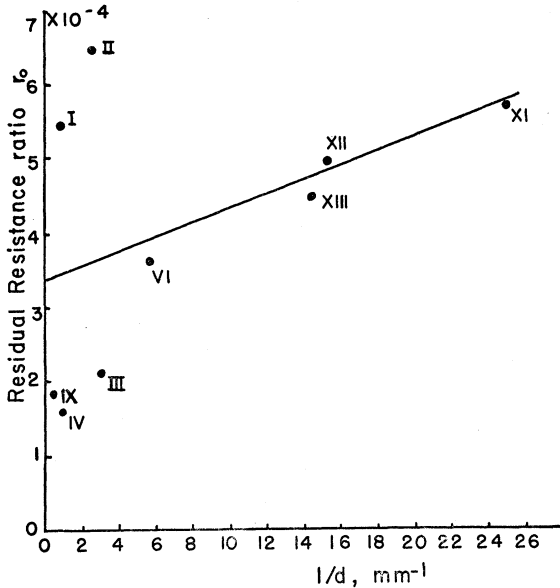


FIG. 1. Residual resistance ratio $r_0=R_0^{\circ K}/R_0^{\circ C}$ as a function of reciprocal diameter. Roman numerals refer to sample numbers.

tion of the reciprocal diameter; the curve is assumed to give the dependence of r_0 on $1/d$ and, using (1), yields a value $al=2.8 \times 10^{-3}$ cm. Assuming an a value of 1 and using $\rho_0^{\circ C}=8.37 \times 10^{-6}$ ohm cm and $r_{00}=3.4 \times 10^{-4}$, we obtain

$$1/\rho l = 12 \times 10^{10} \text{ ohm}^{-1} \text{ cm}^{-2}. \quad (2)$$

III. MEASUREMENT OF RESISTANCE AS A FUNCTION OF THE CURRENT

Figure 2 shows the resistance ratio $r=R(T,I)/R(0^{\circ C}, 0)$ as a function of the current for various temperatures. Curves are displayed for samples IX ($d=1.936$ mm); II ($d=0.608$ mm) and XI ($d=0.038$ mm) which seemed typical of the data obtained.

In Fig. 3, r vs I/I_c plots are shown for the above samples. This type of plot allows more accurate determi-

TABLE II. Temperature dependence.

Sample	$T^{\circ K}$	$10^4 \lim_{I \rightarrow 0} r$	$10^4 r_0$	$10^4 r_T$	$1.99 \times 10^{-2} T^{2.68}$
III	4.213	3.10	2.11	0.99	0.94
	3.402	2.63		0.52	0.53
	2.219	2.28		0.17	0.17
IV	4.213	2.52	1.58	0.94	0.94
	3.402	2.11		0.53	0.53
	2.219	1.72		0.14	0.17
$6.47 \times 10^{-2} T^{2.74}$					
K. Onnes and W. Tuyn	18.11	517.3	335.9	187.4	181.4
	16.45	479.6		143.7	139.2
	14.17	431.7		95.8	92.6
	13.06	410.0		74.1	73.8
	4.19	339.4		3.5	3.29
	3.39	338.7		2.8	1.84

nation of the critical resistance ratio r_c . The curves have been displaced by amounts $I/I_c=0.2$ for the sake of clarity. Without the effective use of the return tube on sample IX, the r vs I/I_c curves were rounded and showed no abrupt rise. This indicates the necessity of having the larger samples free from the stray fields due to the leads.

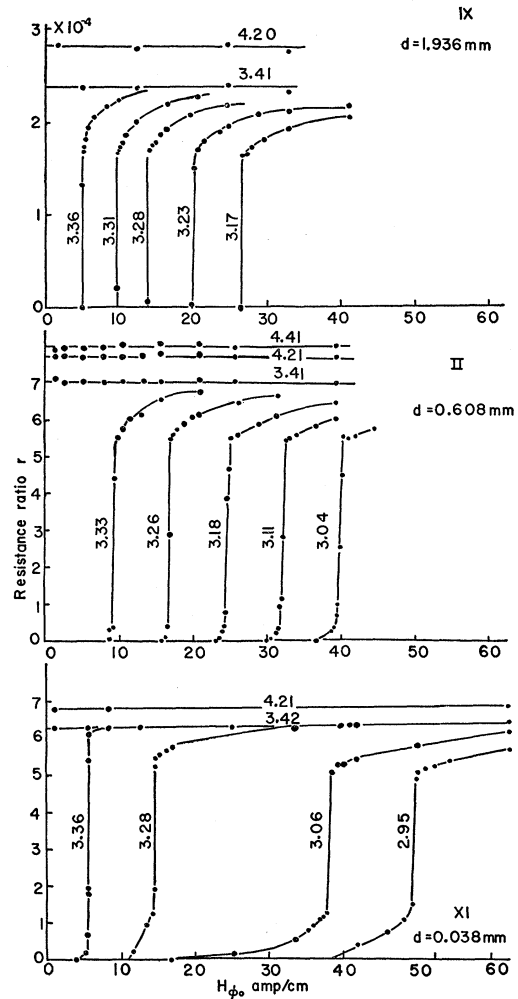


FIG. 2. Resistance ratio r as a function of H_{ϕ_0} , the magnetic field at the surface of the sample due to the current. The numbers on the curves refer to the temperatures.

IV. CRITICAL FIELD CURVE

The critical-field curve for samples I, II, III, and IV is shown in Fig. 4. All samples agree within the accuracy of the measurements (the rest of the samples have been omitted for clarity) and yield a critical temperature of $3.407 \pm 0.005^{\circ K}$ and an initial slope of -110 amp/cm $^{\circ K}$ or -137.6 oe/ $^{\circ K}$. Values of the slope from the literature include -144.0 oe/ $^{\circ K}$ by Misener³ and -155.8 oe/ $^{\circ K}$ by Muench.⁴

³ A. D. Misener, Proc. Roy. Soc. (London) A174, 262 (1940).

⁴ N. L. Muench, Phys. Rev. 99, 1814 (1955).

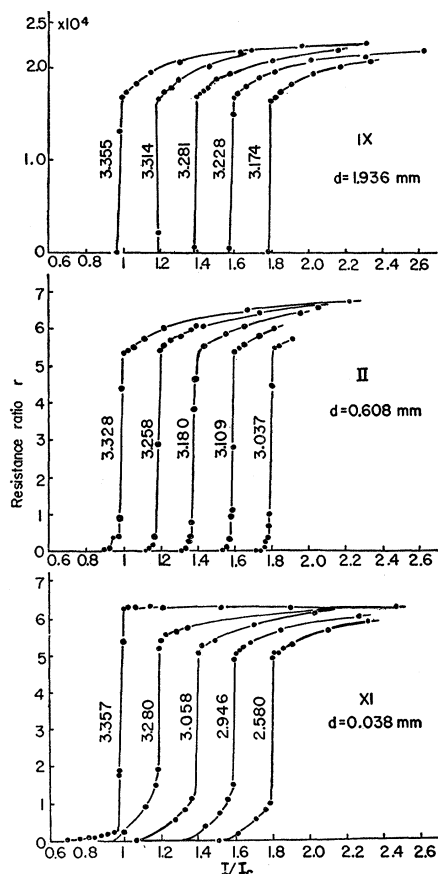


FIG. 3. Resistance ratio r as a function of I/I_c where I_c is the critical current. Successive curves are displaced $I/I_c=0.2$ for the sake of clarity. The numbers on the curves refer to the temperature.

V. TEMPERATURE DEPENDENCE OF RESISTANCE

By using Mathiessen's rule, the temperature dependence was determined as in part V. It was not possible to obtain a good fit with one power law between our data and those of Onnes and Tuyn.⁵ This may be

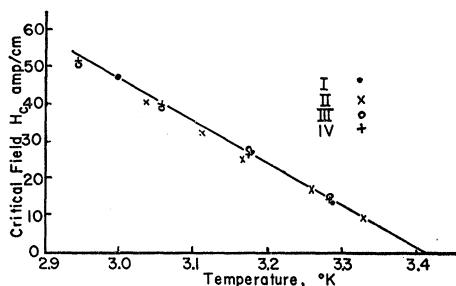


FIG. 4. Critical-field curve for samples I, II, III, and IV. This curve yields a critical temperature of $3.407 \pm 0.005^\circ\text{K}$ and has an initial slope of $-137.6 \text{ oe}/^\circ\text{K}$.

⁵ Kammerlingh Onnes and W. Tuyn, Comm. Leiden Suppl. 16, No. 58, 88 (1926).

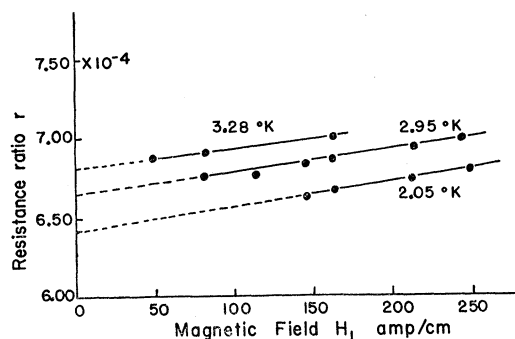


FIG. 5. Increase of resistance ratio in a transverse magnetic field for sample II. Extrapolation in the region where the sample was superconducting is represented by the dotted portion of the curves.

due to the high residual resistance of the Onnes-Tuyn sample ($r_0=335.9 \times 10^{-4}$).

Table II lists the power law chosen for each set of data, and exhibits the quality of the fit obtained. In any case, it is certain that the n , for indium, in the expression

$$r_T = aT^n$$

does not exceed 3.

For the correction of the resistance values, the relation

$$r_T = 1.99 \times 10^{-6} T^{2.68} \quad (3)$$

was used. This dependence also agreed with the average change in resistance from 4.21°K to 3.41°K for samples II, IV, IX, XI, XII, and XIII.

VI. DEPENDENCE OF THE RESISTANCE ON THE MAGNETIC FIELD

The field dependence was measured in order to make corrections for the magnetoresistance as described in part V. A typical curve of r vs perpendicular magnetic field is shown in Fig. 5. From such plots the Kohler diagram in Fig. 6 was obtained, which yields for the

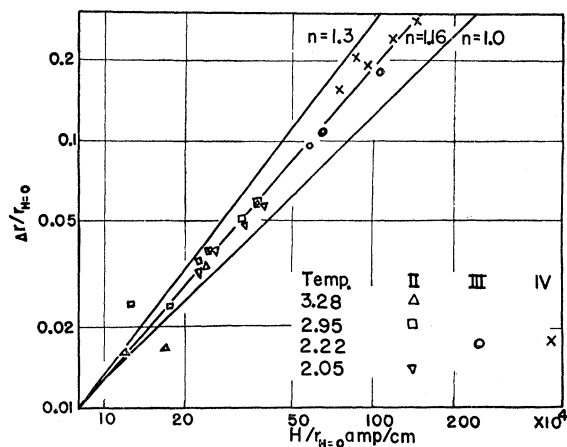


FIG. 6. Kohler diagram for the magnetoresistance of indium in transverse magnetic fields.

best fitting curve:

$$\frac{\Delta r}{r_{H=0}} = 11.7 \times 10^{-4} \left(\frac{H}{r_{H=0}} \times 10^{-4} \right)^{1.16} \quad \text{if } H \text{ is in oersteds,}$$

or

$$\frac{\Delta r}{r_{H=0}} = 8.96 \times 10^{-4} \left(\frac{H}{r_{H=0}} \times 10^{-4} \right)^{1.16}$$

if H is in amperes per cm.

(Although the numbers in this equation are given to 3 figures their accuracy is limited to about $\pm 10\%$.)

II. CORRECTED r_c/r_n VALUES

The values of r_c/r_n were corrected for the temperature and magnetic field dependence of the resistivity of the

TABLE III. Corrected values of r_c/r_n .

Sample	Diameter (mm)	$10^4 r_0$	$T^\circ\text{K}$	$10^4 r_c$	$10^4 r_n$	r_c/r_n
I	1.11	5.46	3.284	4.26 \pm 0.03	5.95	0.75 \pm 0.05
			3.174	4.29 \pm 0.03	5.93	0.723 \pm 0.05
			3.057	4.29 \pm 0.04	5.91	0.726 \pm 0.05
			2.991	4.26 \pm 0.04	5.90	0.722 \pm 0.05
			2.945	4.23 \pm 0.03	5.88	0.719 \pm 0.05
II	0.608	6.46	3.328	5.34 \pm 0.05	6.97	0.766 \pm 0.05
			3.258	5.47 \pm 0.05	6.95	0.787 \pm 0.05
			3.180	5.50 \pm 0.07	6.93	0.794 \pm 0.05
			3.109	5.41 \pm 0.03	6.91	0.783 \pm 0.05
			3.037	5.46 \pm 0.10	6.90	0.791 \pm 0.05
III	0.314	2.11	3.281	1.92 \pm 0.05	2.61	0.736 \pm 0.02
			3.174	1.85 \pm 0.05	2.59	0.714 \pm 0.02
			3.057	1.87 \pm 0.20	2.56	0.730 \pm 0.08
			2.945	1.92 \pm 0.10	2.54	0.756 \pm 0.04
IV	1.140	1.58	3.281	1.48 \pm 0.05	2.08	0.712 \pm 0.02
			3.174	1.43 \pm 0.10	2.06	0.694 \pm 0.04
			3.057	1.46 \pm 0.03	2.04	0.716 \pm 0.02
			2.945	1.50 \pm 0.07	2.03	0.739 \pm 0.04
VI	0.176	3.61	3.284	3.22 \pm 0.10	4.11	0.783 \pm 0.02
			3.174	3.26 \pm 0.10	4.08	0.799 \pm 0.02
			3.126	3.28 \pm 0.10	4.07	0.806 \pm 0.02
			2.947	3.22 \pm 0.10	4.02	0.801 \pm 0.02
			2.049	3.25 \pm 0.10	4.15	0.783 \pm 0.02
IX	1.936	1.84	3.355	1.68 \pm 0.05	2.35	0.715 \pm 0.02
			3.314	1.67 \pm 0.05	2.34	0.714 \pm 0.02
			3.281	1.69 \pm 0.05	2.34	0.722 \pm 0.02
			3.228	1.67 \pm 0.10	2.33	0.717 \pm 0.02
			3.174	1.64 \pm 0.05	2.32	0.707 \pm 0.02
XI	0.038	5.71	3.357	6.28 \pm 0.05	6.22	1.00 \pm 0.02
			3.280	5.45 \pm 0.25	6.20	0.879 \pm 0.04
			3.058	5.08 \pm 0.15	6.16	0.825 \pm 0.03
			2.946	5.09 \pm 0.05	6.13	0.830 \pm 0.02
			2.580	4.93 \pm 0.10	6.07	0.812 \pm 0.02
XII	0.062	4.96	3.357	4.96 \pm 0.05	5.47	0.907 \pm 0.02
			3.281	4.61 \pm 0.07	5.46	0.844 \pm 0.02
			3.058	4.15 \pm 0.15	5.40	0.769 \pm 0.04
			2.946	4.15 \pm 0.15	5.38	0.771 \pm 0.04
			2.580	4.32 \pm 0.03	5.31	0.814 \pm 0.02

normal conducting regions, as in part V, and are listed in Table III.

Heating of the samples was neglected, since the complete discussion contained in part V indicated that the heat transfer coefficient is adequate for such an assumption.

VIII. INFLUENCE OF TEMPERATURE AND MEAN FREE PATH ON THE VALUES OF r_c/r_n

Figure 7(a) shows the values of r_c/r_n plotted vs temperature for samples I, II, and XI. Samples I and II show types of behavior treated in part V. Sample XI, however, shows a sharp rise near the critical temperature; this rise seems to be unique with thin samples (sample XII also shows such a rise).

Values of the mean free path as calculated from Eq. (2) in conjunction with the residual resistance ratios are shown in Table IV for the samples of Scott⁶ and for those used in this investigation.

The values of r_c/r_n shown in Table IV are a weighted average over the plateau values (see part V). Figure 7(b) shows values of r_c/r_n for samples of similar diameter, plotted as a function of the mean free path. The curves are drawn with the guidance of the similar curves for tin, which are also shown. One can see that a larger mean free path leads to smaller values of r_c/r_n for indium as well as tin.

X. INFLUENCE OF SAMPLE DIAMETER ON r_c/r_n

The dependence of the average r_c/r_n on sample diameter is tabulated in Table IV and plotted in Fig. 8

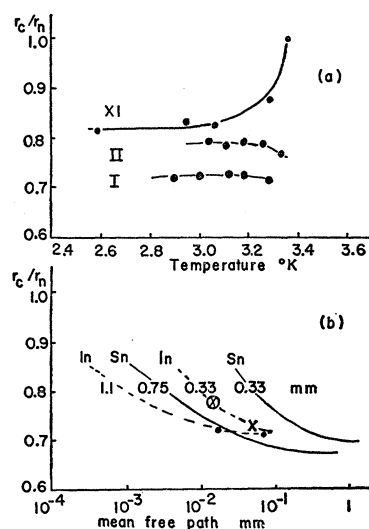


FIG. 7. (a) Dependence of r_c/r_n on temperature. The Roman numerals refer to the sample numbers, these three being selected to exhibit the three types of behavior observed. (b) Dependence of r_c/r_n on electronic mean free path. The circled point was derived from measurements of R. Scott. The curves for tin are taken from reference 1.

⁶ R. B. Scott, J. Research Natl. Bur. Standards **41**, 581 (1948).

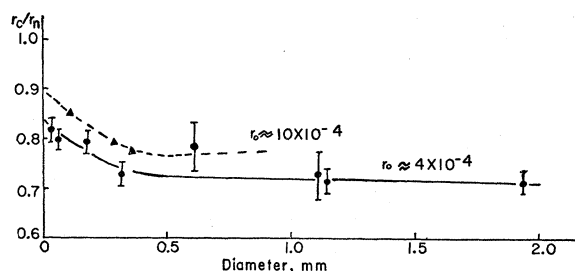


FIG. 8. Dependence of r_c/r_n on diameter of the sample. The symbol \blacktriangle denotes a point taken from the measurements of R. Scott. Approximate residual resistance values are shown on the two curves.

along with Scott's points. The two curves, drawn for different residual resistance ratios, are in accord with the discussion of the influence of mean free path on r_c/r_n . It can be seen that it is very improbable that r_c/r_n goes to 1 for very small diameters, as proposed by Scott,⁶ and the data obtained definitely do not fit Scott's empirical formula even for large diameters.

XI. CONCLUSIONS

The values of r_c/r_n are clearly larger than the theoretical value of 0.5, even for the purest samples of the largest diameter investigated.

The values of r_c/r_n increase markedly with decreasing

TABLE IV. Dependence of r_c/r_n on diameter and electronic mean free path.^a

Sample	Diameter (mm)	Average r_c/r_n	l (mm)
XI	0.038	0.822 ± 0.02	0.276×10^{-1}
XII	0.062	0.799 ± 0.02	0.268
VI	0.176	0.794 ± 0.02	0.308
III	0.314	0.728 ± 0.02	0.508
II	0.608	0.784 ± 0.05	0.151
I	1.11	0.721 ± 0.05	0.176
IV	1.140	0.715 ± 0.02	0.626
IX	1.936	0.715 ± 0.02	0.522
Scott			
1	0.106	0.854	0.0734
2	0.286	0.795	0.0854
3	0.357	0.778	0.117

^a The electronic mean free path is calculated for impurity scattering only, with a correction for the effect of boundary scattering.

electronic mean free path. This increase is larger for samples of smaller diameter.

The values of r_c/r_n apparently do not go to 1 at small diameters and become approximately constant for samples of large diameter.

XII. ACKNOWLEDGMENTS

The authors are indebted to Professor G. H. Dieke for the provision of the liquid helium. They wish to thank the National Science Foundation for supporting this work by a grant. Thanks are also due Mr. R. Sarup for reproducing the drawings of this report.